Modeling Study of the Sorption-Enhanced Reaction Process for CO2 Capture. II.

Application to Steam-Methane Reforming

H.T.J. Reijers

J. Boon

G.J. Elzinga

P.D. Cobden

W.G. Haije

R.W. van den Brink

Published in the Ind. Eng. Chem. Res., 2009,48 (15) pp 6975-6982

ECN-W--09-041 December 2009

Modeling Study of the Sorption-Enhanced Reaction Process for CO_2 Capture. II. Application to Steam-Methane Reforming

Hendricus Th. J. Reijers,* Jurriaan Boon, Gerard D. Elzinga, Paul D. Cobden, Wim G. Haije, and Ruud W. van den Brink

Hydrogen & Clean Fossil Fuels, Energy research Centre of The Netherlands, P.O. Box 1, 1755 ZG, Petten, The Netherlands

In this paper, the reactor model introduced in part I will be verified using the results of an analytical solution for the increase of CH_4 conversion over the bed and validated using the results of sorption-enhanced steam-methane reforming laboratory-scale experiments. An experimentally derived rate equation for the steam-methane reforming reaction is used, a literature rate equation for the water−gas shift reaction. An overview of modeling work on the sorption-enhanced reaction process for steam-methane reforming performed by other groups is presented. The CH_4 and CO_2 profiles obtained from laboratory-scale experiments are quite satisfactorily described using a Freundlich isotherm. A sensitivity analysis shows that both the CH_4 and CO_2 profiles are sensitive to the adopted isotherm model and its parameters. In addition to that, the CH_4 and CO_2 profiles are sensitive to the diffusion coefficient. Neither profile is sensitive to the particle size or the heat of adsorption.

Introduction

This paper is a continuation of the work on the SESMR (sorption-enhanced steam-methane reforming) reactor model started in part I of this series.[1] The background of the work was given in part I and will be briefly summarized here.

The sorption-enhanced reaction process (SERP) offers an attractive possibility for precombustion CO_2 capture. The hydrogen is produced in the reformer according to the steam-methane reforming (SMR) reaction

$$CH_4 + H_2O \leftrightarrow CO + 3H_2 \quad (\Delta H^\circ_{298} = +206\ \text{kJ/mol}) \tag{1}$$

and the water−gas shift (WGS) reaction

$$CO + H_2O \leftrightarrow CO_2 + H_2 \quad (\Delta H^\circ_{298} = -41\ \text{kJ/mol}) \tag{2}$$

A suitable sorbent is mixed with the SMR catalyst. The CO_2 produced is selectively removed by the sorbent. Thus, the reaction equilibria shift to the product side, enabling the SMR and WGS reactions and the CO_2 capture processes to be combined in one single step. The same CH_4 conversion may be obtained at much lower temperatures, say between 723 and 823 K, than in conventional SMR without sorbent, which is performed typically between 1123 and 1223 K. Clearly, the process is a batch process requiring a regeneration step to remove the adsorbed CO_2.

The research by Air Products in the 1990s showed that hydrotalcite (HTC) promoted with K_2CO_3 and denoted as kHTC worked satisfactorily as CO_2 adsorbent in the temperature range 673−773 K.[4,5] The purpose of this paper is the validation of the model using the results of laboratory-scale SESMR experiments. In part I, the results of CO_2 sorption experiments were applied for that purpose. An overview of modeling work on the sorption-enhanced reaction process for steam-methane reforming performed by other groups is presented. After that, the model is verified using an analytical solution for the increase of CH_4 conversion over the bed, and validated using the experimentally determined CH_4 and CO_2 profiles. The only authors who have made a comparison between experimental data and simulated curves for SESMR are Ding and Alpay.[5] However, they did this for only one set of conditions, and their experimental CH_4 and CO_2 curves show only two and six data points, respectively, before the equilibrium values are obtained. The experiments shown here expand on this work.

Just as for the sorption-only experiments, the sensitivity of the calculated adsorption profiles for the isotherm parameters and several other parameters is evaluated. The conditions for the desorption step are identical in both sets of experiments. For that reason, the desorption profiles are left out here.

Reaction Rate Equations

The model needs expressions of the reaction rate equations for the steam-methane reforming (SMR) and water−gas shift (WGS) reactions, eqs 1 and 2. Here, the expression for the kinetics of the SMR reaction being first order in CH_4 derived by Wei and Iglesia has been adopted:[2]

$$R_{SMR} = k_{SMR} p_{CH_4} \exp\left(-\frac{E_{SMR}}{RT}\right)\left(1 - \frac{p_{H_2}{}^3 p_{CO}}{p_{CH_4} p_{H_2O}} \frac{1}{K_{SMR}}\right) \tag{3}$$

with

$$K_{SMR} = \exp(Z(Z(Z(0.12849Z - 0.20333) - 0.57487) + 27.0096) - 3.2195)(\text{bar}^2) \tag{4}$$

in which

$$Z = \frac{1000}{T} - 1 \tag{5}$$

and where T is expressed in kelvin. This expression gave a sufficiently accurate description of the experimentally obtained CH_4 conversions using the fitted values of k_{SMR} and E_{SMR}. The WGS reaction could be considered at equilibrium. The WGS

* To whom correspondence should be addressed. Tel.: +31 (0) 224-564588. Fax: +31 (0) 224-568489. E-mail address: reijers@ecn.nl.

10.1021/ie8013204 CCC: $40.75

Table 1. Parameters of Reaction Rates

reaction	pre-exponential factor k	activation energy E
SMR	9×10^2 mol/kg-cat·Pa·s	9×10^4 J/mol
WGS	1.3×10^6 mol/kg-cat·Pa$^{0.05}$·s	8.6×10^4 J/mol

equilibrium is approximated by using an expression for fast WGS kinetics, derived for a platinum/ceria/alumina catalyst by Germani et al.[3] for the temperature range 573−673 K

$$R_{WGS} = k_{WGS} \exp\left(-\frac{E_{WGS}}{RT}\right) p_{CO}{}^{0.13} p_{H_2O}{}^{0.49} p_{CO_2}{}^{-0.12} p_{H_2}{}^{-0.45} \times \left(1 - \frac{p_{CO_2} p_{H_2}}{p_{CO} p_{H_2O} K_{WGS}}\right) \quad (6)$$

with

$$K_{WGS} = \exp(Z(Z(-0.18210Z + 0.563176) + 4.189249) + 0.341737) \quad (7)$$

Xu and Froment needed the reaction rate of a third reaction being the sum of eqs 1 and 2 to describe their experimental data satisfactorily.[6] In contrast to that, it was found here that the experimentally determined gas compositions could be described well at all applied conditions, using only eqs 3 and 6 for the SMR and WGS kinetics, respectively.

The values of the pre-exponential factors (k_{SMR} and k_{WGS}) and the activation energies (E_{SMR} and E_{WGS}) are shown in Table 1. Since Wei and Iglesia determined k_{SMR} and E_{SMR} for the temperature range 873−1073 K, we have fitted eq 3 to our data and determined these parameters for the temperature range 523−773 K, which covers the operation temperature of our experiments. Values of k_{WGS} and E_{WGS} could not be determined because the WGS reaction proceeded so quickly over this catalyst compared to the SMR reaction, that it could be considered to be in instantaneous equilibrium. For that reason, results are not sensitive to the parameter values of the WGS reaction rate equation. We used the values determined by Germani et al. yielding reaction rates which are 1−2 orders of magnitude larger than the reaction rate of eq 3.

Parameter Values

Table 2 shows the values of the bed parameters used in the code, and Table 3, the values of the step durations, feed gas conditions and wall temperature. The bed parameters are the same as in part I of this series, with the following additional remarks. The adsorbent-catalyst bed is situated between $z = 0.124$ m and $z = 0.16$ m here. The range of values in which the binary diffusion coefficients D_{ij} vary, for those gas pairs that include H_2 ($3-6 \times 10^{-4}$ m^2/s) clearly differs from the D_{ij} range for the gas pairs without H_2 ($0.5-1.4 \times 10^{-4}$ m^2/s); see the Supporting Information of part I.[1] Therefore, two values of D_m were used: one for H_2 and one for the other components.

For the calculation of the total bed porosity, the contribution of the particle porosity ε_p is required. An average value of ε_p was determined by taking the average over the two kinds of particles as follows:

$$\varepsilon_p = \frac{\sum_i \varepsilon_{p,j} V_{p,j}}{\sum_i V_{p,j}} \quad (8)$$

Table 2. Parameters of Reactor Bed

quantity	meaning	value
ε_b (−)	bed porosity	0.40
ε_p (−)	(average) particle porosity	0.32
ε_t (−)	total porosity	0.59
d_p (m)	particle diameter	3.15×10^{-4}
d_t (m)	tube diameter	0.016
h (m)	packed bed height	0.036
k_g (W/m·K)	thermal conductivity of gas-phase	0.025
k_p (W/m·K)	thermal conductivity of particle	1
μ (kg/m·s)	viscosity of gas phase	2.87×10^{-5}
$C_{p,sol}$ (J/kg·K)	heat capacity of solid (= catalyst and adsorbent)	850
ΔH_{ads} (J/mol)	heat of adsorption	−17000
D_m (m^2/s)	molecular diffusivity of all gases except of H_2	1.2×10^{-4}
D_{m,H_2} (m^2/s)	molecular diffusivity of H_2	3.5×10^{-4}
$D_{p,ads}$ (m^2/s)	diffusivity of CO_2 within adsorbent particle due to pore diffusion	7.7×10^{-7}
$D^0_{s,ads}$ (m^2/s)	diffusivity of CO_2 within adsorbent particle due to surface diffusion at zero coverage of the pores	1.5×10^{-10}
$\rho_{b,cat}$ (kg/m^3)	bulk density of catalyst	417
$\rho_{b,ads}$ (kg/m^3)	bulk density of adsorbent	306
$\rho_{p,ads}$ (kg/m^3)	particle density of adsorbent	922
η_j	effectiveness factor	1

Table 3. Conditions of Steps A, B, C, and D

	A	B	C	D
t_{step} (s)	600	10	4480	10
y_{CO_2}	0	0	0	0
y_{CH_4}	0.058	0	0	0
y_{H_2O}	0.172	0.29	0.29	0.29
y_{N_2}	0.77	0.71	0.71	0.71
u_f (m/s)	0.0047	0.0047−0.0187	0.0187	0.0187−0.0047
p_f (Pa)	1.01325×10^5	1.01325×10^5	1.01325×10^5	1.01325×10^5
T_f (K)	673	673	673	673
T_w (K)	673	673	673	673

where $V_{p,j}$ is the particle volume (the subscript j denotes an adsorbent or a catalyst particle), given by

$$V_{p,j} = \frac{m_j}{\rho_{p,j}} \quad (9)$$

Here, $\varepsilon_{p,j}$ and $\rho_{p,j}$ are the porosity and density, respectively, of a particle of type j, and m_j is the total weight of particles of type j in the bed. Their values are given in Table 4, together with the values of the bulk density ρ_b, solid density ρ_s, the bed porosity ε_b, and the pore volume V_{pore}, determined from N_2 measurements. The bulk densities $\rho_{b,ads}$ and $\rho_{b,cat}$ are determined from the known adsorbent and catalyst weights and the packed bed volume.

Other Modeling Work

Below, the modeling work for sorption-enhanced SMR (SESMR) performed by other groups is briefly reviewed. Table 5 provides a summary. In the column called *deviations* in Table 5, deviations from the model used in this paper are specified. Most of the models discussed below have been applied to large-scale reactors at elevated pressures (5−20 bar) and temperatures between 673 and 773 K for HTC-based sorbents. Typically, the characteristic quantities that are calculated, include the conversion of CH_4 or CO, the H_2 productivity (the amount of hydrogen produced in mol per weight unit of solid, where solid refers to both catalyst and sorbent), the concentration of

Table 4. Particle Densities and Porosities

	m (g)	ρ_b (g/cm^3)	ε_b (−)	ρ_p (g/cm^3)	V_{pore} (cm^3/g)	ε_p (−)	ρ_s (g/cm^3)	V_p (cm^3/g)
adsorbent	2.2	0.553	0.401	0.922	0.076	0.071	0.994	2.39
catalyst	3.0	0.643	0.401	1.072	0.492	0.529	2.270	2.80

Table 5. Modeling Studies for SESMR in a Fixed Bed

group	sorbent	deviations	investigated issue
Imperial College, London[4,5]	kHTC	DA isotherm, XF kinetics	parameter variation
University Porto, Portugal[7]	kHTC	DA isotherm, XF kinetics	comparison of two process cycles.
University Porto, Portugal[9]	kHTC		five-step cycle
University Porto, Portugal[10]	kHTC		division of reactor bed into three subsections having different adsorbent:catalyst weight ratios
University Porto, Portugal[11]	kHTC	DA isotherm, XF kinetics, intraparticle diffusion	effect of intraparticle diffusion
Lehigh University, USA[18,19]	kHTC	no axial dispersion, no pressure loss, CO_2 concentration independent k_{LDF}	compare TSSER with PSSER, sensitity analysis
Lehigh University, USA[20]	kHTC, Na_2O-promoted alumina		apply TSSER to WGS with CO_2 removal, compare sorbents
Lehigh University, USA[21]	Na_2O-promoted alumina		apply TSSER to WGS with CO_2 removal, investigate effect reaction temperature
NTNU, Norway[15]	Li_2ZrO_3	heterogeneous, adsorbent kinetics, friction term, intraparticle diffusion	two-particle vs one-particle heterogeneous model, reactor performance
NTNU, Norway[16]	Li_4SiO_4	heterogeneous, adsorbent kinetics, friction term, intraparticle diffusion	two-particle vs one-particle heterogeneous model, reactor performance, comparison with fluidized bed
KIER, Korea[13]	CaO	adsorbent kinetics, no axial dispersion	reactor performance
University Manchester, UK[22]	kHTC	heterogeneous, catalyst/adsorbent distribution within particle	parameter variation, effect of different catalyst/adsorbent distributions within particle on H_2 yield

impurities (CH_4, CO, and CO_2) in the product gas, the steam duty (amount of steam in moles required to regenerate the sorbent bed, expressed per mole produced H_2 or per mole recovered CO_2), and the CO_2 recovery (the fraction of all carbon that goes into the reactor as CH_4, CO, or CO_2, and that is captured as CO_2) if CO_2 capture is aimed at.

In two papers, Ding and Alpay (Imperial College, England) investigated CO_2 sorption-only[4] and SESMR,[5] both experimentally and by modeling. The experimentally derived expression for the CO_2 adsorption isotherm[4] has been used by most other groups who performed similar modeling work and is denoted as the *DA isotherm* in Table 5. For the reaction kinetics of the SMR and WGS reactions, the expressions derived by Xu and Froment for a $Ni/MgAl_2O_4$ catalyst[6] were used, denoted as *XF kinetics*. It was found that the CH_4 conversion enhancement increased when the space time or operation pressure was increased, or the steam/CH_4 ratio was decreased.[5] The experimentally observed elution profiles for sorption-only and SMR could be well-described by the model presented in the paper.[4,5]

The group of Rodrigues (University of Porto, Portugal) have published several papers on SESMR. In the first of these, two simulated, four-step process cycles for a 6 m long reactor bed using pressure swing for regeneration were compared.[7] The one cycle was performed at the same temperature during all steps of the cycle (723 K). The other cycle differs from the first one in that a lower temperature (673 K) was used during the first part of the purge step. During the lower-temperature part of the purge step, 10% H_2 was added to the purge gas. The effect of these measures (lower temperature and H_2 present in purge gas) is that the desorption of CO_2 is enhanced due to the reverse WGS and methanation reactions, resulting in a higher H_2 productivity. In particular, lower eluent CO concentrations were obtained (<30 ppm), suitable for fuel cell application, at the expense of the H_2 productivity (25 to 33% lower). In the same paper, the calculated H_2 productivity and CH_4 conversion using the constant temperature cycle were compared with the experimental data of Air Products and Chemicals.[8] Differences of approximately 25% were found. In another paper, a five-step cycle was investigated in which the purge step was split in two steps: one using CH_4 as purge gas to push the gaseous CO_2 out of the reactor bed and another step using H_2 product gas for further regeneration of the bed.[9] The temperature was constant during all steps (723 K). The model developed before[7] was used to predict the behavior of a 2 m long reactor bed. It took about 15 cycles before a steady state was obtained, characterized by a CH_4 conversion of 64%, an H_2 productivity of 0.63 mol/kg-solid, and an H_2 purity of 80%. The CO_2 mole fraction of the effluent during the two purge steps varied between 13 and 3%, making the system unsuitable for simultaneous CO_2 removal. In another paper, a reactor bed of 6 m length was divided into three sections, the middle section having a twice as high adsorbent:catalyst weight ratio (4:1) as the inlet and outlet sections (2:1).[10] Two cases were compared: the case where the temperature is uniform in all sections and equal to 733 K (case 1) and the case where the temperature in the outlet section is 693 K (case 2), so that CO traces are better removed by WGS. The differences between the two cases were remarkable: even though the CH_4 conversions and H_2 productivities were comparable in both cases, the CO and CO_2 concentrations in the product gas of case 2 are 5 to 10 times smaller than in case 1. In another paper, the effect of intraparticle diffusion in both adsorbent and catalyst on the CH_4 conversion and H_2 productivity was investigated and compared with the results of simulations without intraparticle diffusion.[11] For the simulations with intraparticle diffusion, the CH_4 conversions and H_2 productivities were a few percent higher than obtained from those without intraparticle diffusion.

In a series of papers, Lee et al. (Korea Institute of Energy Research) investigated the reaction kinetics for CO_2 sorption by CaO and applied it subsequently to a fixed bed and moving bed reactor for steam reforming with in situ CO_2 removal.[12−14] In the models that were developed in the same papers, axial dispersion was not taken into account. Not a linear driving force (LDF) model, but a quadratic driving force (QDF) model was applied to describe the kinetics of the carbonation reaction.[12] The catalyst:adsorbent weight ratio was 18:82. Only the

adsorption step was studied. The optimal operation temperature was found to be around 923 K. Lower temperatures would result in a too low carbonation rate, while higher temperatures yielded too high CO concentrations in the product gas. The H_2 productivities were around 4 mol H_2/kg-solid, thus an order of magnitude larger than typical values for reactors with kHTC as sorbent (see, e.g., the work of Rodrigues mentioned above and references). On the other hand, the CO_2 and CO impurities were an order of magnitude larger in the CaO-based systems. It was concluded, therefore, that CaO-based SESMR systems are unsuitable for production of fuel-cell grade hydrogen gas as long as any CaO-based sorbent with a considerable working capacity much lower than 923 K has not been developed.

The group of Jakobsen (Norwegian University of Science and Technology (NTNU), Norway) performed some fixed-bed simulations for Li_2ZrO_3 and Li_4SiO_4 as sorbent.[15,16] Instead of the Ergun friction terms, a different friction term in the pressure balance equation was applied, valid for $500 < Re_p/(1-\varepsilon_b) < 60\,000$ where Re_p is the particle Reynold's number and ε_b the bed porosity.[17] Both a pseudohomogeneous model and a heterogeneous model were used, the latter model both for one and for two particles taking intraparticle diffusion into account. In the two-particle model, the sorbent and catalyst particles are considered as different particles, whereas in the one-particle model both functions are in the same particle. As a consequence, intraparticle diffusion limitation effects become only apparent in the two-particle model, not in the one-particle model. For Li_2ZrO_3, intraparticle diffusion was not noticeable because the slow kinetics of the CO_2 sorption reaction dominated the overall CO_2 sorption rate. For Li_4SiO_4, the CO_2 sorption kinetics was much better and mass transport limitation effects due to intraparticle diffusion only occurred for particle sizes larger than 5 mm. From a comparison between a fixed-bed and fluidized-bed reactor follows the finding that that longer reactor beds are needed in the fluidized-bed reactor to obtain the same conversion as in the fixed-bed reactor.

At Lehigh University (PA, USA), the group of Sircar[18−21] is actively working on the TSSER (temperature swing sorption-enhanced reaction) concept, both experimentally and by process simulations, and both for SESMR and SEWGS (sorption-enhanced water−gas shift) systems. As the name implies, the sorbents they are testing (kHTC and Na_2O-promoted alumina) are regenerated by temperature swing. The regeneration temperature is between 823 and 863 K. TSSER involves longer cycle times than PSSER because heating the reactor bed from reaction to regeneration temperature takes more time than changing the pressure in the bed as in PSSER. This drawback is outweighed by several advantages such as the following: storage of sensible heat in the bed during regeneration that is used in the succeeding reaction step, a higher working capacity of the sorbent, and a large pressure increase of the CO_2 product during temperature swing.

Simulations have been done for SESMR using a 2 m long reactor bed[18] and compared with experimental data obtained for the pressure swing sorption-enhanced reaction (PSSER) process by Air Products and Chemicals.[8] The calculated H_2 productivity and CH_4 conversion were clearly better for TSSER (0.39 mol/kg and 96%, respectively) than the experimental values for PSSER (0.25 mol/kg and 73%, respectively). Also, the sensitivity of various process variables was investigated, showing that there is an optimum catalyst:adsorbent weight ratio (8−10 wt % catalyst) and H_2O:CH_4 molar ratio of the feed gas (6 mol H_2O/mol CH_4).[19] The performance deteriorated when the pressure was increased, whereas it was unaffected when the feed gas temperature varied between 623 and 763 K. The latter is due to the large amount of sensible heat stored in the bed during regeneration. In two other papers, they applied TSSER to WGS systems, focusing not only on H_2 production, but also on CO_2 removal. The four-step cycle process used for TSSER-based SMR was extended with a rinse step taking place after the reaction step. In the first of these papers, kHTC was compared with Na_2O-promoted alumina at a reaction temperature of 673 K.[20] It was found that, although its H_2 productivity was 15% less, the alumina-based sorbent required 44% less purge steam than kHTC due to its more favorable adsorption isotherm and slightly better desorption kinetics in comparison with kHTC. In the second paper on SEWGS, the effect of reaction temperature on performance was studied, keeping the regeneration temperature the same (823 K).[21] It was found that the H_2 productivity was improved by 38% by decreasing the reaction temperature from 673 to 473 K, leaving the CO_2 recovery nearly unchanged. Table 6 shows the H_2 productivities, CO_2 recoveries, CO conversions, and purge steam demands expressed as the H_2O/CO_2 molar ratio for the above-mentioned four cases (kHTC vs Na_2O-doped alumina at 673 K and Na_2O-doped alumina at a reaction temperature of 473 vs 673 K), calculated for a pressure of 15 atm, a regeneration temperature of 823 K, and a feed gas composition of 20% CO and 80% H_2O. Cycle times and gas flow rates of the first two cases (kHTC vs Na_2O-doped alumina at 673 K) differed from those of the other two cases (Na_2O-doped alumina at a reaction temperature of 473 vs 673 K). The CO_2 purities are nearly 100% in all cases.

Table 6. Calculated Results for a TSSER-Based WGS System at a Pressure of 15 atm and a Regeneration Temperature of 550 °C for a 20% CO/80% H_2O Feed Gas

sorbent	reac temp[a] (K)	CO conv[b] (%)	H_2 prod[c] (mol/kg)	CO_2 rec[d] (%)	H_2O/CO_2 (mol/mol)
kHTC, alumina[20]	673	93.3	0.710	57.1	18.1
	673	91.5	0.601	63.4	10.1
alumina[21]	673	91.3	0.585	72.9	12.4
	473	91.0	0.807	71.1	14.4

[a] Reaction temperature. [b] Conversion. [c] Productivity. [d] Recovery.

Recently, Kapil et al. used a heterogeneous model taking intraparticle diffusion into account.[22] This allowed investigation of the variation of the adsorbent:catalyst weight ratio over the particle volume. It was found that when this ratio gradually increased from shell to core region within the particle, a better H_2 yield was obtained than when the adsorbent and catalyst were uniformly distributed over the particle volume.

Verification

Verification was performed by comparing the increase of CH_4 conversion over the bed calculated by the code with that obtained from an analytical solution for a homogeneous catalyst bed. The following starting points were used apart from the assumptions mentioned under Reactor Model in part I of this series:[1]

- the feed gas contains only CH_4, H_2O, and N_2,
- CO_2 adsorption does not occur,
- pressure p and temperature T are constant throughout the bed,
- axial dispersion does not occur,
- the reaction rate equation of the steam-methane reforming reaction given by eq 3 applies, and
- water−gas shift is at equilibrium. The CH_4 conversion X is related to the catalyst weight W_{cat} and CH_4 flow F_{CH_4} fed to the bed as follows[23]

$$\frac{W_{cat}}{F_{CH_4}} = \int_0^x \frac{dx}{R_{SMR}(x)} \tag{10}$$

where R_{SMR} is given by eq 3. To evaluate the integral, the partial pressures in eq 3 must be expressed in x. If y is the CO conversion, it can be readily shown that

$$p_{CH_4} = \frac{1 - x}{1 + N + S + 2x} p$$

$$p_{H_2O} = \frac{S - x - y}{1 + N + S + 2x} p$$

$$p_{H_2} = \frac{3x + y}{1 + N + S + 2x} p \tag{11}$$

$$p_{CO} = \frac{x - y}{1 + N + S + 2x} p$$

and

$$p_{CO_2} = \frac{y}{1 + N + S + 2x} p$$

where S and N are the H_2O/CH_4 and N_2/CH_4 molar ratios, respectively. After substitution of eqs 11 in eq 3 and using

$$K_{SMR} = \frac{(3x + y)y}{(S - x - y)(x - y)} \tag{12}$$

the integral eq 10 can be solved for X. Since

$$\frac{W_{cat}}{F_{CH_4}} = \frac{\rho_{b,cat} z RT}{u y^0_{CH_4}} \tag{13}$$

where $\rho_{b,cat}$ is the bulk catalyst density, z is the bed length, R is the gas constant, T is the temperature, and u and $y^0_{CH_4}$ are the superficial velocity and the CH_4 mole fraction of the feed gas. X can be solved as function of z. Figure 1 shows the variation of the CH_4 conversion over the bed calculated by the Matlab model and obtained from eqs 10−13 using $y^0_{CH_4} = 0.01$, $S = 3$, $N = 96$, $\rho_{b,cat} = 453$ kg/m^3, $T = 673$ K, $p = 1$ bar, and $u = 0.0047$ m/s, which are more or less typical conditions for the experiments reported here. The agreement is excellent. Both curves approach the equilibrium CH_4 conversion of 53% toward the end of the bed.

Experimental Section

Details of the laboratory-scale experiments can be found in part I of this paper.[1] For sample preparation, the same sieve fraction (0.212−0.425 mm) was used for both adsorbent and catalyst, which were mixed together in the reactor as homogeneously as possible. The same adsorbent as used for the experiments of part I, was applied here: PURAL MG70, impregnated with 22 wt % K_2CO_3 and obtained from SASOL. Details of the preparation can be found in a previous paper.[24] The reactor was loaded with equal weights of catalyst and adsorbent materials, 6 g in total. Though the initial weights were equal, the final weights were not due to further calcination of the adsorbent. This resulted in a final total weight of approximately 5.2 g, which was assumed to be due to weight loss of the adsorbent only. The feed consisted of CH_4 and H_2O in a certain mol:mol ratio, referred to as the steam-to-carbon ratio S/C, the balance of gases was provided by N_2. Regeneration of the adsorbents was performed with 29% H_2O in N_2 in cocurrent direction. In Table 7, the standard experimental conditions are summarized, corresponding to S/C = 3.

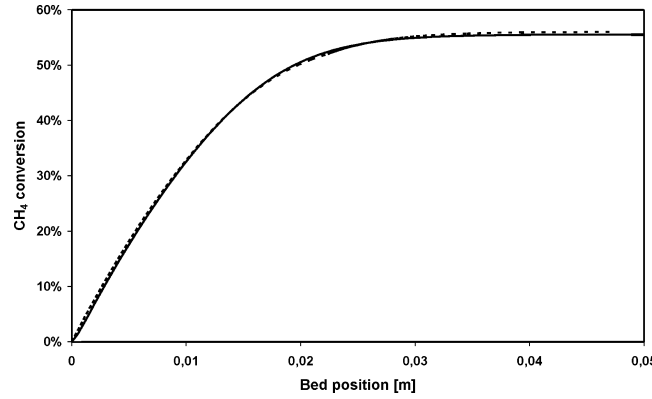

Figure 1. Variation of CH_4 conversion over the catalyst bed calculated by the Matlab model (solid line) and the analytical solution (dashed line) using $y^0_{CH_4} = 0.01$, $S = 3$, $N = 96$, $\rho_{b,cat} = 453$ kg/m^3, $T = 673$ K, $p = 1$ bar, and $u = 0.00468$ m/s.

Table 7. Standard Experimental Conditions for SESMR Experiments

	feed step	regeneration step
flow (mL/min)	25	100
composition (%)		
CH_4	5.8	
H_2O	17.2	29
N_2	77	71
T (K)	673	673
duration (min)	10	75
adsorbent weight (g)	2.2	
catalyst weight (g)	3.0	
particle size (mm)	0.212−0.425	

The SMR catalyst was a precommercial sample supplied by a vendor under a nondisclosure agreement. The reactor could be bypassed for calibration of the gases. Water was removed from the exit gases before analysis was performed. Sampling by a gas chromatograph for CO_2, CH_4, H_2, and CO occurred every 105 s during the SESMR experiments.

Numerical Simulation

Details of the numerical simulation can be found in the Supporting Information of part I.[1] As discussed there, the experimental data must be corrected for the time it takes for the feed gas to travel from the mass flow controller to the reactor inlet and for the time it takes for the outlet gas to travel from the reactor outlet to the gas chromatograph. These corrections have been taken into account as follows. The time in the simulations and the time in the experiments, respectively, t_{sim} and t_{exp}, are related as $t_{sim} = t_{exp} - 73$ s for the feed step and as $t_{sim} = t_{exp} - 15$ s for the regeneration step.

Sorption-Enhanced Experiments

Figures 2 and 3 show the experimental and simulated results of an SESMR experiment. Different isotherms, based on the Freundlich and Langmuir isotherm models, were used for the simulations. Table 8 shows the values of the isotherm parameters. As for CO_2 sorption-only, the Langmuir results are clearly worse than those of the Freundlich based simulations. The Freundlich-based simulation in Figure 2 is used as the *reference* and referred to as such throughout this paper. Figures 4 and 5 show the results of a series of SESMR experiments in which the S/C ratio has been varied, together with the corresponding

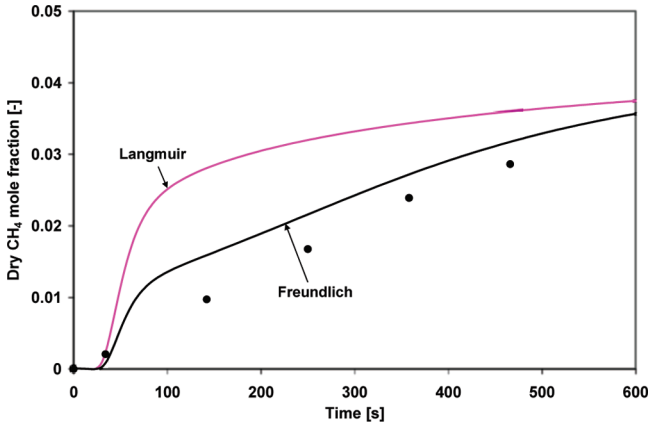

Figure 2. Dry CH_4 mole fraction at reactor outlet during adsorption for various isotherms, compared with experimental results (•): conditions 673 K, 5.8% CH_4, 17.2% H_2O, and 77% N_2, 25 mL/min.

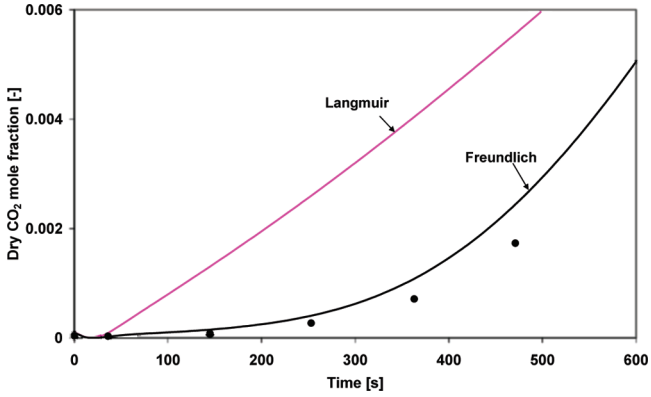

Figure 3. Dry CO_2 mole fraction at reactor outlet during adsorption for various isotherms, compared with experimental results (•): conditions 673 K, 5.8% CH_4, 17.2% H_2O, and 77% N_2, 25 mL/min.

Table 8. Fit Parameters for the Langmuir and Freundlich isotherms

	Langmuir isotherm		Freundlich isotherm	
	parameter	value	parameter	value
data fit	m (mol/kg)	0.475	k (mol/kg)	0.700
	b (Pa^{-1})	3.78×10^{-4}	$1/n$ (−)	0.301
upper estimate	m (mol/kg)	0.538	k (mol/kg)	0.807
	b (Pa^{-1})	3.93×10^{-4}	$1/n$ (−)	0.303
lower estimate	m (mol/kg)	0.412	k (mol/kg)	0.596
	b (Pa^{-1})	3.67×10^{-4}	$1/n$ (−)	0.297

simulations. The steam mole fraction in the feed gas was kept constant (0.172) while the CH_4 mole fraction was adjusted such that S/C varied between 2 and 6. Increasing the S/C ratio results in higher CH_4 conversion and thus a lower CH_4 mole fraction at the reactor outlet. The short horizontal lines at the right side of Figure 4 denote the equilibrium values of the dry CH_4 mole fraction when no adsorbent is present. For all cases, the equilibrium values are higher than the CH_4 mole fractions at the end of the adsorption step because the sorbent is not completely saturated. The dry CO_2 mole fractions at equilibrium without adsorbent are between 2.1% at S/C = 2 and 1.7% at S/C = 6 and, thus, outside the range of mole fractions shown in Figure 5. The simulated data follow the experimentally observed trend: at higher S/C ratio or similarly at lower CH_4 mole fraction in the feed since the steam content was kept constant, the curves move downward, both for the CH_4 and CO_2.

The temperature variation over the bed located between the dashed lines is shown in Figure 6. Its behavior is determined by two processes: the endothermic steam-methane reforming

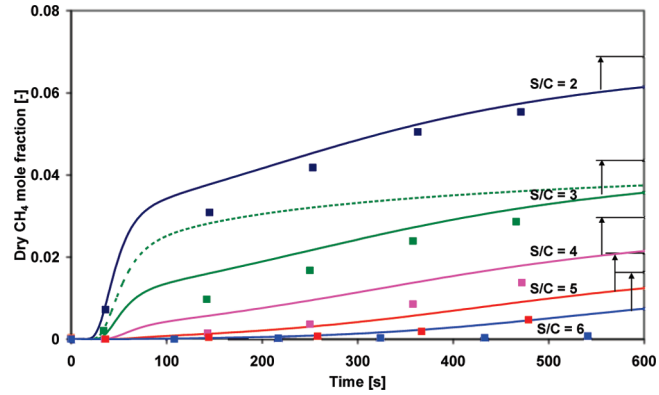

Figure 4. Dry CH_4 mole fraction at reactor outlet during adsorption for various S/C ratios: experimental data (symbols) and simulated data (solid lines). The dashed line is based on the Langmuir isotherm at S/C = 3. The short horizontal lines at the right denote equilibrium values, coupled by arrows to the appropriate simulated line: conditions 673 K, variable CH_4 concentration, 17.2% H_2O, balanced by N_2, 25 mL/min.

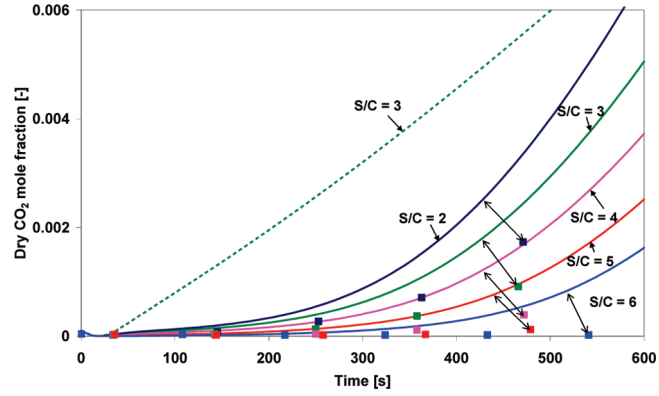

Figure 5. Dry CO_2 mole fraction at reactor outlet during adsorption for various S/C ratios: experimental data (symbols) and simulated data (solid lines). The dashed line is based on the Langmuir isotherm at S/C = 3: conditions 673 K, variable CH_4 concentration, 17.2% H_2O, balanced by N_2, 25 mL/min.

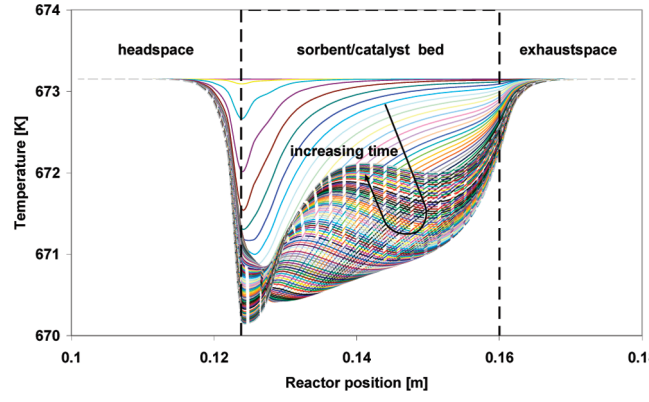

Figure 6. Variation of temperature over the reactor during adsorption for S/C = 3: conditions 673 K, 5.8% CH_4, 17.2% H_2O, and 77% N_2, 25 mL/min.

reaction and the exothermic adsorption of CO_2. At first, the bed is empty and adsorption takes place throughout the whole bed as does steam-methane reforming. Because the negative heat of reaction of the steam-methane reforming reactions exceeds the positive heat of adsorption of CO_2, the temperature decreases. As the bed fills, the CO_2 removal rate of the adsorbent slows down, as does the steam-methane reforming reaction rate. The temperature increases in the whole bed, except for the inlet

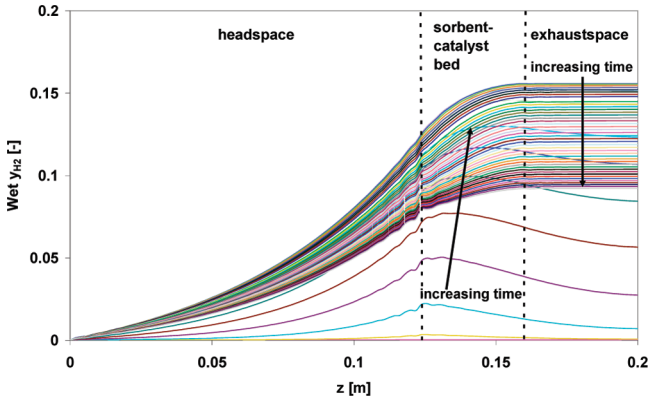

Figure 7. Variation of the wet H_2 mole fraction over the reactor during adsorption for S/C = 3: conditions 673 K, 5.8% CH_4, 17.2% H_2O, and 77% N_2, 25 mL/min.

Table 9. Parameter Values for the Sensitivity Study

varied parameter	lower value	higher value
particle size d_p (m)	2.12×10^{-4}	4.25×10^{-4}
molecular diffusion coefficient D_m (m^2/s)	5.28×10^{-5}	13.6×10^{-5}
ΔH_{ads} (kJ/mol)		115

part where the equilibrium steam-methane reforming reaction concentrates as would be the case without adsorbent. Since the maximum temperature decrease is only 3 K, there is no need to apply a two-dimensional model here.

Figure 7 shows the simulated variation of the (wet) H_2 mole fraction over the reactor during adsorption. Note the strong backward diffusion of H_2 to the empty inlet part of the reactor. The time evolution of the profiles is determined by two factors: SERP and the approach to equilibrium. At the beginning of the adsorption step, the curves move upward because the SMR reaction starts and all adsorbent sites are available. As the adsorbent fills, the sorption-enhancement is reduced, and at a certain time (t = 96 s), the profiles start to move downward until the equilibrium mole fraction is obtained. As discussed in part I of this series, the effects of diffusion observed here are much less important in large-scale reactors due to the combined effects of elevated pressure and higher flow rate, and because of the larger bed length.

Sensitivity Analysis

As for the CO_2 sorption-only simulations, a sensitivity study was performed for SESMR simulations by varying several parameters of the reference:

- isotherm parameters,
- particle size d_p,
- molecular diffusion coefficient D_m, and
- ΔH_{ads}. Table 8 shows the upper and lower estimated values of the isotherm parameters, and Table 9, the values of the other parameters used for the sensitivity study. The values of d_p were determined by the lower and upper limits of the sieve fraction, and those of D_m by the minimum and maximum values of the calculated diffusion coefficients of pairs of molecules. Figures 8−11 show the results of the sensitivity study: Figures 8 and 9 show those for CH_4, and Figures 10 and 11, those for CO_2. Only the results of the adsorption step are shown since the effects on the desorption step have been studied in part I of this series.[1] The results of both CH_4 and CO_2 are sensitive to variation of the isotherm and to increasing D_m, much less sensitive to changing d_p. Increasing ΔH_{ads} or decreasing D_m does not influence the shape of the CH_4 and CO_2 profiles. For that reason, these profiles are not shown.

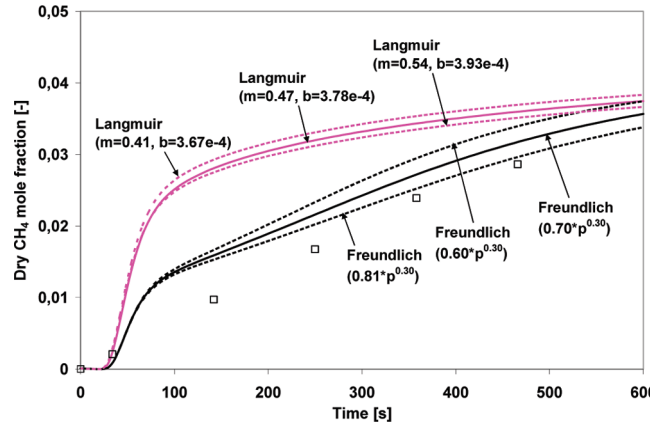

Figure 8. Dry CH_4 mole fraction at reactor outlet during adsorption for sorption-enhanced steam reforming of methane: sensitivity study results for Freundlich and Langmuir isotherm parameters. The symbols are experimental data: conditions 673 K, 5.8% CH_4, 17.2% H_2O, and 77% N_2, 25 mL/min.

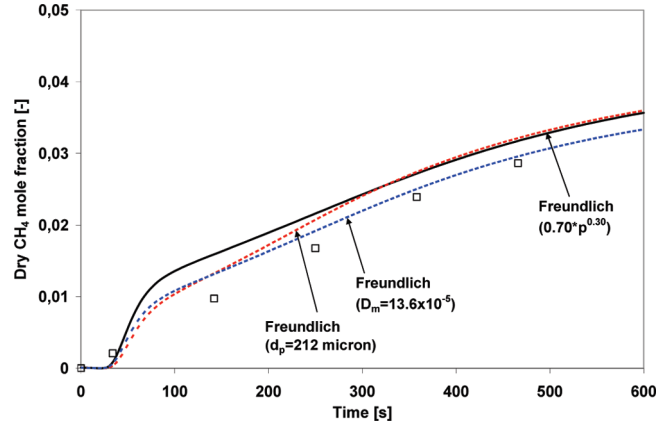

Figure 9. Dry CH_4 mole fraction at reactor outlet during adsorption for sorption-enhanced steam reforming of methane: sensitivity study results for d_p and D_m. The symbols are experimental data: conditions 673 K, 5.8% CH_4, 17.2% H_2O, and 77% N_2, 25 mL/min.

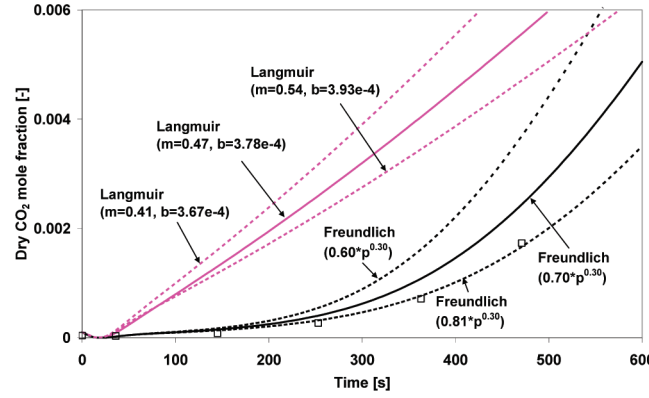

Figure 10. Dry CO_2 mole fraction at reactor outlet during adsorption for sorption-enhanced steam reforming of methane: sensitivity study results for Freundlich and Langmuir isotherm parameters. The symbols are experimental data: conditions 673 K, 5.8% CH_4, 17.2% H_2O, and 77% N_2, 25 mL/min.

Conclusions

In both parts of this series, the one-dimensional model for a fixed bed SERP reactor has been validated using the results of

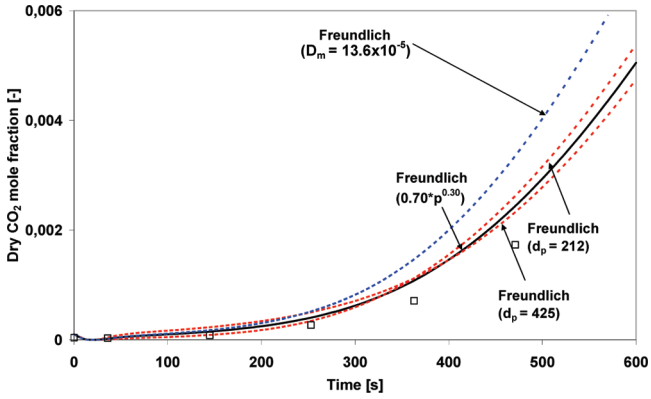

Figure 11. Dry CO_2 mole fraction at reactor outlet during adsorption for sorption-enhanced steam reforming of methane: sensitivity study results for d_p and D_m. The symbols are experimental data: conditions 673 K, 5.8% CH_4, 17.2% H_2O, and 77% N_2, 25 mL/min.

laboratory-scale experiments. When comparing this work with related modeling studies in the literature, it follows that other groups have mostly focused on the simulation of large-scale reactors without thorough validation. This work tries to fill this gap. The parameter values required by the model were not treated as fit parameters, but measured by ourselves (densities, porosities, SMR kinetics) or were taken from the literature. The following conclusions can be drawn:

1. The measured concentration profiles of CH_4 or CO_2 of sorption-enhanced steam-methane reforming experiments can be well-described by a Freundlich isotherm. Just as for the CO_2 sorption-only experiments, the Langmuir adsorption isotherm does not describe the experimental data so well as the Freundlich adsorption isotherm.

2. The increase of CH_4 conversion over the bed calculated by the Matlab model and an analytical solution for the same conditions agree well.

3. At the conditions of the laboratory-scale experiments considered here, the CH_4 and CO_2 concentration profiles are sensitive to changes of the Freundlich isotherm parameters and, to less degree, to changes of the particle size, molecular diffusion coefficient, or the heat of adsorption of CO_2. The good agreement between experiments and simulations gives confidence in the suitability of the model for predicting the performance of large-scale reactors. As next step, we plan to simulate a large-scale SEWGS reactor for CO_2 capture. The effect of among others cycle times, operating conditions, and catalyst−sorbent ratio on CO conversion, CO_2 purity, and CO_2 recovery will be investigated. A paper on experimental data of this reactor has in fact been recently published.[25]

Acknowledgment

This research has been carried out by ECN in the CATO-project. CATO (Carbon Capture, Transport and Storage) is the Dutch national research program on CO_2 Capture and Storage (www.co2-cato.nl). The Dutch government supports CATO with 50% subsidy from the BSIK program of the Ministry of Economic Affairs.

Literature Cited

(1) Reijers, H. Th. J.; Boon, J.; Elzinga, G. D.; Cobden, P. D.; van den Brink, R. W. Modeling Study of the Sorption-Enhanced Reaction Process for CO_2 Capture. I. Model Development and Validation. *Ind. Eng. Chem. Res.*; http://dx.doi.org/10.1021/ie8013204.

(2) Wei, J.; Iglesia, E. Structural requirements and reaction pathways in methane activation and chemical conversion catalyzed by rhodium. *J. Catal.* **2004**, *225*, 116–127.

(3) Germani, G.; Alphonse, P.; Courty, M.; Schuurman, Y.; Mirodatos, C. Platinum/ceria/alumina catalysts on microstructures for carbon monoxide conversion. *Catal. Today* **2005**, *110*, 114–120.

(4) Ding, Y.; Alpay, E. Equilibria and kinetics of high temperature CO_2 adsorption on hydrotalcite adorbent. *Chem. Eng. Sci.* **2000**, *55*, 3461–3474.

(5) Ding, Y.; Alpay, E. Adsorption-enhanced steam-methane-reforming. *Chem. Eng. Sci.* **2000**, *55*, 3929–3940.

(6) Xu, J.; Froment, G. F. Methane steam reforming, methanation and water-gas shift: I. Intrinsic kinetics. *AIChE J.* **1989**, *35*, 88–96.

(7) Xiu, G.; Li, P.; Rodrigues, A. E. Sorption-enhanced reaction process with reactive regeneration. *Chem. Eng. Sci.* **2002**, *57*, 3893–3908.

(8) Waldron, W. F.; Hufton, J. R.; Sircar, S. Production of Hydrogen by Cyclic Sorption Enhanced Reaction Process. *AIChE J.* **2001**, *47*, 1477–1479.

(9) Xiu, G.; Soares, J. L.; Li, P.; Rodrigues, A. E. Simulation of five-step one-bed sorption-enhanced reaction process. *AIChE J.* **2002**, *48*, 2817–2832.

(10) Xiu, G.; Li, P.; Rodrigues, A. E. New generalized strategy for improving sorption-enhanced reaction process. *Chem. Eng. Sci.* **2003**, *58*, 3425–3437.

(11) Xiu, G.; Li, P.; Rodrigues, A. E. Adsorption-enhanced steam-methane reforming with intraparticle-diffusion limitations. *Chem. Eng. Sci.* **2003**, *93*, 83–93.

(12) Lee, D. K. An apparent kinetic model for the carbonation of calcium oxide by carbon dioxide. *Chem. Eng. J.* **2004**, *100*, 71–77.

(13) Lee, D. K.; Baek, I. H.; Yoon, W. L. Modeling and simulation for the methane steam reforming enhanced by in situ removal utilizing the CaO carbonation for H_2 production. *Chem. Eng. Sci.* **2004**, *59*, 931–942.

(14) Lee, D. K.; Baek, I. H.; Yoon, W. L. A simulation study for the hybrid reaction of methane steam reforming and in situ CO_2 removal in a moving bed reactor of a catalyst admixed with a CaO-based CO_2 acceptor for H_2 production. *Int. J. Hydr. Energy* **2006**, *31*, 649–657.

(15) Rusten, H. K.; Ochoa-Fernández, E.; Chen, D.; Jakobsen, H. A. Numerical Investigation of Sorption Enhanced Steam Methane Reforming Using Li_2ZrO_3 as CO_2-acceptor. *Ind. Eng. Chem. Res.* **2007**, *46*, 4435–4443.

(16) Rusten, H. K.; Ochoa-Fernández, E.; Lindborg, H.; Chen, D.; Jakobsen, H. A. Hydrogen Production by Sorption-Enhanced Steam Methane Reforming Using Lithium Oxides as CO_2-Acceptor. *Ind. Eng. Chem. Res.* **2007**, *46*, 8729–8737.

(17) Hicks, R. E. Pressure drop in packed beds of spheres. *Ind. Eng. Chem. Fundam.* **1970**, *9*, 500–502.

(18) Lee, K. B.; Beaver, M. G.; Caram, H. S.; Sircar, S. Novel Thermal-Swing Sorption-Enhanced Reaction Process Concept for Hydrogen Production by Low-Temperature Steam-Methane Reforming. *Ind. Eng. Chem. Res.* **2007**, *46*, 5003–5014.

(19) Lee, K. B.; Beaver, M. G.; Caram, H. S.; Sircar, S. Production of fuel-cell grade hydrogen by thermal swing sorption enhanced reaction concept. *Int. J. Hydr. Energy* **2008**, *33*, 781–790.

(20) Lee, K. B.; Beaver, M. G.; Caram, H. S.; Sircar, S. Performance of Na_2O promoted alumina as CO_2 chemisorbent in sorption-enhanced reaction process for simultaneous production of fuel-cell grade H_2 and compressed CO_2 from synthesis gas. *J. Power Sources* **2008**, *176*, 312–319.

(21) Lee, K. B.; Beaver, M. G.; Caram, H. S.; Sircar, S. Effect of temperature on the performance of Thermal-Swing Sorption-Enhanced Reaction Process for simultaneous production of fuel-cell grade H_2 and compressed CO_2 from synthesis gas. *Ind. Eng. Chem. Res.*, submitted for publication.

(22) Kapil, A.; Bhat, S. A.; Sadhukhan, J. Process Systems Engineering Multiscale characterization framework for sorption enhanced reaction processes. *AIChE J.* **2008**, *54*, 1025–1036.

(23) Levenspiel, O. Chapter 5: Single Ideal Reactors. In *Chemical Reaction Engineering*; Wiley: New York, 1972.

(24) Reijers, H. Th. J.; Valster-Schiermeier, S. A. E.; Cobden, P. D.; van den Brink, R. W. Hydrotalcite as CO_2 Sorbent for Sorption-Enhanced Steam Reforming of Methane. *Ind. Eng. Chem. Res.* **2006**, *45*, 2522–2530.

(25) Van Selow, E. R.; Cobden, P. D.; Verbraeken, P. A.; Hufton, J. R.; van den Brink, R. W. Carbon Capture by Sorption-Enhanced Water-Gas Shift Reaction Process using Hydrotalcite-based Material. *Ind. Eng. Chem. Res.* **2009**, *48*, 4194–4201.

Received for review September 1, 2008
Revised manuscript received February 27, 2009
Accepted May 27, 2009

IE8013204